Synthesis of hcp-Co Nanodisks.

Victor F Puntes, Daniela Zanchet[†], Can K Erdonmez[‡] and A Paul Alivisatos**

Chemistry Department and [‡]Materials Science Department, UC Berkeley, 94720

Berkeley, USA

[†]LME, Laboratorio Nacional de Luz Sincrotron, Campinas, Brazil.

*vfpuntes@ffn.ub.es, alivis@uclink4.berkeley.edu

ABSTRACT. hcp Co disk-shaped nanocrystals were obtained by rapid decomposition of cobalt carbonyl in presence of linear amines. Other surfactants, in addition to the amines, like phosphine oxides and oleic acid were used to improve size dispersion, shape control and nanocrystal stability. Co disks are ferromagnetic in character and they spontaneously self assemble into long ribbons. X-ray and electron diffraction, electron microscopy and SQUID magnetometry have been employed to characterize this material.

1. INTRODUCTION

We present a method for the preparation of disk shaped Co nanocrystals. The control of nanocrystal shape remains an interesting and important topic in nanoparticle research (due to the coupling between shape and properties at the nanometer scale [1]), and several approaches are being pursued. We previously presented results for nanocrystals of CdSe and Co, in which the selective adsorption of organic surfactants onto particular crystallographic facets is employed as a means of controlling the shape. The concept of selective adsorption is to use an organic molecule to inhibit the growth of a particular crystallographic direction. Since the rate constants for growth are exponentially dependent upon surface energy, small energy differences can be exploited to yield major anisotropies in the kinetic limit. Note that in this case, the thermodynamic limit will still yield nearly spherically shaped particles. Here we show a more comprehensive picture of shape control via selective adsorption in the Co system. These results are of interest from the point of view of understanding nanocrystal growth, but also because of the interesting magnetic, electrical, optical, and catalytic properties of the resulting Co based materials.

Our interest is in discovering unifying principles where the underlying mechanisms of nanocrystal shape control via selective adsorption follow a pattern in several different systems, similar to the well-known case of vapor-liquid-solid growth [2]. Such examples are of importance given the recent observation of several surprising cases of shape control of inorganic nanocrystals, which are rather difficult to explain. For instance, there is the observation of Wang and coworkers that ribbons of metal oxides can be grown using the SLS method [3]. Likewise, Park and coworkers have observed that rods of ferroelectric nanocrystals of $BaTiO_3$ are obtained in a single surfactant in what is believed to be a single solvent micellar system [4]. This occurs despite the fact that the

elongation is along the 100 direction, for which there are three symmetry equivalent faces. Thus, there may be many avenues for symmetry breaking and shape control at work in both gas phase and solution phase methods. One possibility suggested by Peng for solution phase shape control is that a momentary fluctuation may lower the surfactant coverage on a particular face, allowing that face to grow rapidly, depleting the local monomer concentration. It has been suggested that this could set up a self-sustaining gradient in monomer that continuously acts to feed more monomer to the growing facet [5]. Banfield and coworkers [6] and more recently Weller et al. [7] have discussed the concept of oriented attachment, in which anisotropic shapes are obtained by selective fusion of faceted nanocrystals along particular directions. Similar results have been found in Pt particles collapsing to form wires [8] and iron nanorods [9]. Other disk-like nanoparticles have been recently reported on the literature [10].

Of current interest in the literature of nanocrystal shape control is the case of Co. Co possesses multiple crystal structures (hcp, fcc, and epsilon [11,12]) that are close in energy, suggesting that surfactant adhesion or modest variation in temperature may be used to control the crystal phase, size and shape, and thus, ultimately determine the physical and chemical properties. In this paper we extend our earlier work on the synthesis of Co nanocrystals via the thermal decomposition of $Co_2(CO)_8$ in a mixture of hot organic solvent and surfactants [13]. We report conditions of temperature and surfactant composition for which there is a high yield of anisotropic nanocrystals. Second, we demonstrate that the anisotropically shaped nanocrystals we reported earlier and that we confirm now, are in fact hcp disks and not rods as previously thought. The disks appear in TEM to be rods due to their propensity to form stacks that

lie on their side, which in TEM projection resemble rods. Disk formation is generally expected from selective adsorption models, where growth along a unique axis is inhibited (which is the inverse of rod formation). The resulting materials form a wide range of interesting super-assemblies due to the balance among different interaction mechanisms.

2. MATERIALS AND METHODS

Co nanocrystal synthesis was carried out using standard airless procedures and commercially available reagents. As a source for Co atoms, di-cobalt octa-carbonyl $Co_2(CO)_8$ was used. A solution containing the carbonyl was injected into a mixture of hot organic solvent and surfactants. $Co_2(CO)_8$ decomposes at 50 °C in inert atmosphere (and 25 °C in air leading to CoO and $Co(OH)_2$). The decomposition of $Co_2(CO)_8$ is complex and normally goes through intermediates like $Co_4(CO)_{12}$ and $Co_6(CO)_{16}$, which are black crystalline solids, and other unstable mononuclear Co carbonyls. At higher temperatures, $Co_2(CO)_8$ is fully decomposed to Co. For example, at 100 ºC, complete decarboxylation takes over 2h. However, much faster decomposition is observed at 150 ºC and it is over in about one minute at 200 ºC [14]. The evolution of the decomposition of the cobalt carbonyl can be monitored by FTIR spectroscopy following the distinct CO vibration peak.

Di-cobalt octa-carbonyl $Co_2(CO)_8$ containing 1-5% hexane as a stabilizer, oleic acid (OA, 99%), anhydrous o-dichlorobenzene (DCB, 99%), dodecyl amine (DDA, 99%), tetradecylamine (TDA, 99%), hexadecylamine (HDA, 99%), octadecylamine (ODA, 99%), tri-butylamine (TBA, 99%) and tri-octylamine (TOA, 99%) were purchased from Aldrich. Tri-octylphosphine oxide (TOPO, 90%) was purchased from Alfa Aesar. While oleic acid, $Co_2(CO)_8$ and DCB were kept in the drybox, TOPO and the amines were stored under air.

A typical synthesis consisted of: degassing with Ar 0.1 g TOPO in a three-neck flask for 20 min; introduction of 15 ml of DCB + 0.1 ml OA under Ar;

heating to reflux temperature (~182 °C); rapid injection of 0.54 g of $Co_2(CO)_8$ diluted in 3 ml of DCB (precursor solution); lowering of the temperature a few hundred seconds later; and extraction of the solution. Note that in order to dissolve the cobalt precursor, solutions are normally vigorously shaken for 30 minutes in a vortex apparatus. There is often a solid residue that does not go in solution suggesting that the $Co_2(CO)_8$/DCB solution is close to saturation. For the rest of the reactions presented in this paper, only the surfactant mixture (combination of OA, TOPO and an amine) and the reaction time are modified. Details for the reactions may be found in Table 1 (see end of the text). This one step reaction takes between one and twenty minutes yielding a concentrated (10^{14} to 10^{16} particles per milliliter) black ferrofluid.

After the reaction, to clean the excess of surfactant or extract the nanocrystals, an equivalent volume of anhydrous MeOH is added to the original solution and centrifuged for 5 minutes. After that, a black magnetic powder is recovered, which can be re-dissolved with other non-polar solvents. MeOH and rapid centrifugation is sometimes too aggressive and strips the surfactant layer, leading to irreversible aggregation of the nanocrystals. EtOH and isopropanol destabilize the solutions less, resulting in slower precipitation, and yielding readily re-dispersible nanocrystals. Adding small amounts (~0.05 ml) of a long chain (C_n, $n \geq 11$) alcohol at the end of the reaction helps to coat any exposed crystal surface, improving passivation against oxidation and solubility in non-polar solvents.

Powder X-ray diffraction was performed using Co Kα radiation (1.790 Å) and a general area detector (GADDS, Bruker). The instrument resolution is 0.05º in 2θ and the accumulation time for each sample was at least 20 minutes. XRD samples were prepared by depositing a precipitated powder on a quartz plate or introducing the grounded powder in a 0.5 mm quartz capillary. XRD patterns were also simulated and a detailed description of the procedure may be found in the supplementary material.

Nanocrystal size, morphology, structure and superstructures were probed by Transmission Electron Microscopy (TEM) at the National Center for Electron Microscopy at the Lawrence Berkeley National Laboratory, on a JEOL CX200 and a 002b Top Con electron microscope (200 kV) and at the LME-Brazilian National Synchrotron Laboratory on a JEM-3010 (300 kV). A drop of the colloids (2% weight of particles in the volume) was put onto a carbon-coated TEM grid at room temperature and slowly evaporated (covered with a watch glass). The use of high boiling solvents, like DCB, allows slow evaporation at RT, which permits the particles to diffuse to their lowest energy sites during evaporation, producing well-defined super-structures. To enhance the TEM contrast, some of the images are slightly out of focus in order to see Fresnel fringes surrounding the grains.

SQUID magnetometry was employed to characterize the magnetic structure. Samples were diluted (up to 10^{11}-10^{12} particles per ml, which corresponds to an average interparticle distance of 350 nm), in order to avoid dipolar interactions. To select the concentration, normalized magnetization

curves were measured as a function of the concentration until they superimposed, indicating that there is no more concentration related effect observed. Samples were sealed under Ar in a glass container and measured at 200 K (o-DCB melting point is -17 C) after zero and field (1 Tesla) cooling from room temperature.

3. RESULTS

The injection of $Co_2(CO)_8$ into hot DCB, in the presence of OA, yields spherically shaped ε–Co nanocrystals with a relatively broad size distribution (10-20% variation in diameter, Fig.1a). As we reported earlier, the addition of TOPO changes the results in two ways. In the presence of TOPO, anisotropically shaped Co nanocrystals (disks) are formed, in the earliest moments (~10 seconds) after the growth begins (Fig.1b). If the reaction is quenched at this point, a high yield of disks can be obtained; however, it is difficult to quench the reaction so quickly. If the reaction is allowed to continue at the growth temperature, the disks are rapidly redissolved as the temperature (T) rises up from the initial drop produced by the injection. A few minutes later, a very narrow size distribution of spherically shaped nanocrystals are formed (3-5% variation in diameter, Fig.1c). This can be explained if the TOPO acts both as a selective absorber, altering the relative growth rates of different faces of the crystals, as well as a molecule that promotes atom exchange with the monomer reservoir during growth (enabling size distribution focusing).

Here, we report that it is much easier to prepare disks in the presence of linear amine surfactants, as opposed to TOPO. In the presence of amines, the yield of disks is higher (Fig.2), and the disks persist for much longer periods of time following injection (tens of minutes), although if the system remains hot for long enough, the thermodynamically stable ε-Co spheres are eventually obtained. It is interesting to note how a collection of two different narrow distributions, hcp-disks and ε-Co spheres, with different size, shape and crystal structure, are

simultaneously obtained. Disk yields are further increased when: i) larger amounts of surfactant are introduced or ii) the amine is co-injected with the cobalt precursor. In addition, the presence of TOPO in the surfactant mixture further improves the size distribution of the disks (Fig.3).

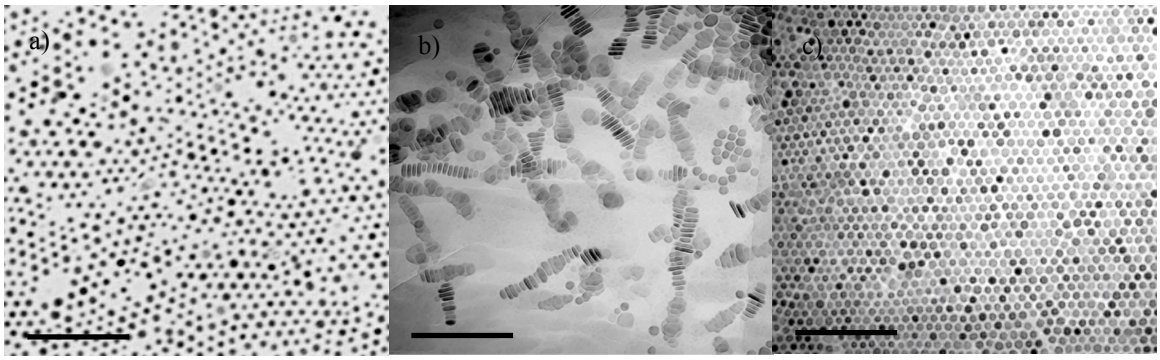

Fig.1. TEM pictures of Co NC (left to right) synthesized (a) after refluxing for 5 min in the presence of oleic acid, (b) in the presence of both oleic acid and TOPO at 10 sec, and (c) in the presence of both oleic acid and TOPO at 5 min.

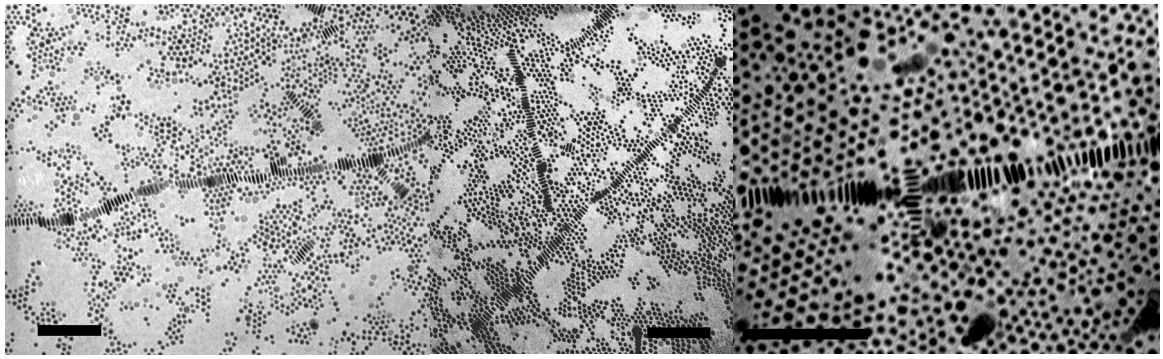

Fig.2. TEM pictures of Co NC synthesized in the presence of oleic acid and octadecylamine. Bars are 100 nm.

By adjusting the conditions of the reaction and time, it is possible to adjust the relative populations of the ε-Co spheres and the hcp-Co disks (up to a yield 85% of disks). However, in order to obtain a pure fraction of hcp-Co disks containing no spheres, it is necessary to physically separate the two populations after the reaction is quenched. Given the major differences in their magnetic properties, magnetic separation is the easiest method to isolate hcp-Co disks. The magnetic separation can be performed by exposing the colloidal mixture to a 1T magnetic field, followed by re-dispersion of the ferrofluids by vigorous shaking and then rapid collection of a fraction on the side of the vial with a 300 Oe magnet. This yields pure ribbons of stacked hcp-Co disks. The magnetic separation works best for disks of a particular size (around 4x30 nm). If the disks are too small, they are as soluble as the ε-Co spheres, and if they are too large, the disks rapidly and permanently aggregate (along with some spheres).

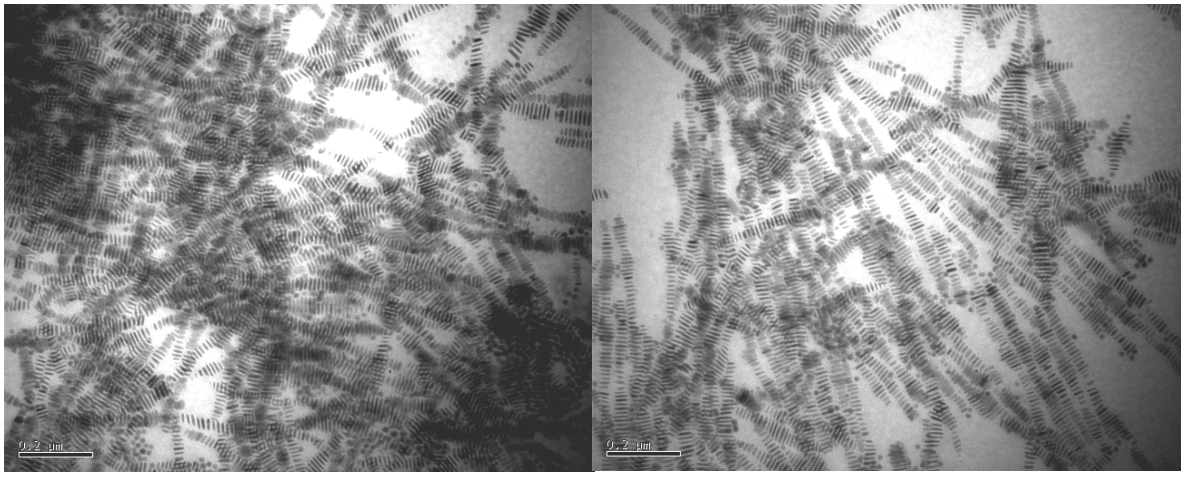

Fig.3. TEM of Co nanodisks assemblies standing on its edge. Bars are 200 nm.

TEM studies of disk samples show long ribbons of disks stacked face-to-face and lying on edge. In the 2D TEM images, these assemblies closely resemble ribbons of rods. To verify the disk shape, tilting experiments have been performed which show that the standing disks varied in thickness when tilted in the short direction and remained of constant length when tilted in the long one.

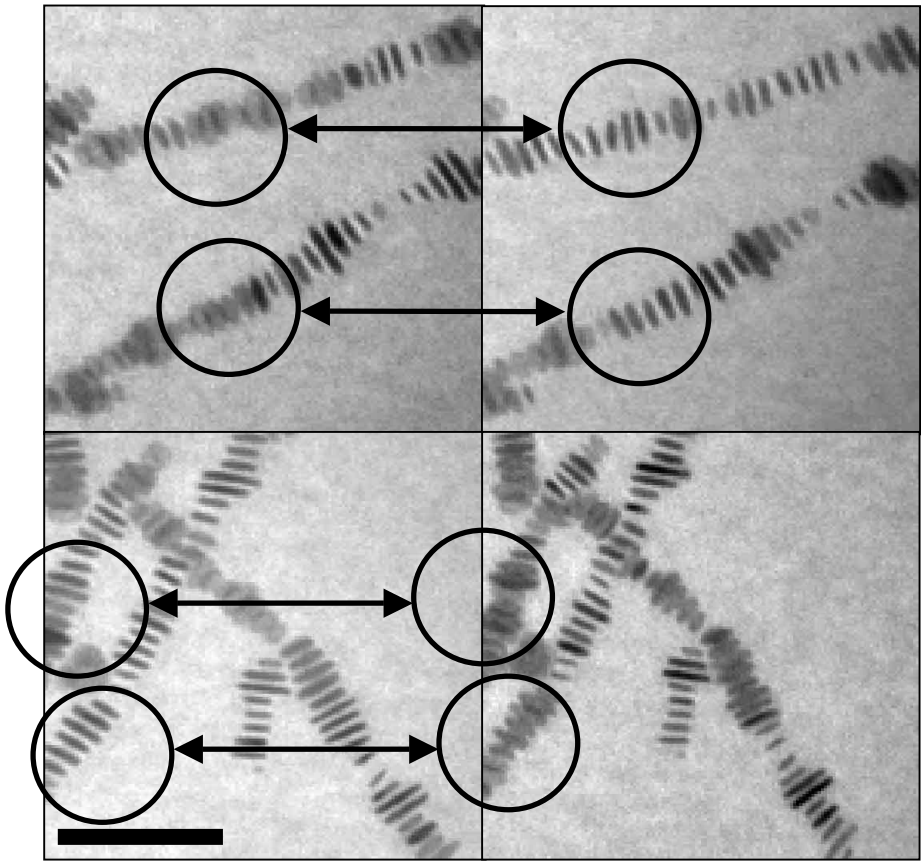

Fig.4 TEM picture of standing disk, the pictures on the left correspond to no tilt, the pictures on the right correspond to 25° tilt. The bar is 200 nm. Tilting direction correspond with the double arrows.

This is shown in Fig.4. Not all the disks rotate at the same time in the same direction (the substrate, amorphous carbon film, is not flat) suggesting the possibility of rocking when tilted. In cases where disks lie flat on the TEM substrate, it is still possible to distinguish between flat disks and spheres due to the relatively low contrast of a large diameter disk compared to a sphere of the same radius. In addition, when disks and spheres are simultaneously present, the two populations show markedly different size distributions. Thus, in Fig.2, for spheres <d>~10 nm, while for disks <d>~25 nm. TEM studies further suggest that the nanodisks are single crystals as observed in the diffraction contrast of the TEM pictures, dark field images, and high resolution TEM (HRTEM) images (see complementary material).

X-ray powder diffraction experiments (Fig.5) and simulations on Co nanocrystal powders (Fig.6) confirm the TEM assignments. We have simulated the X-ray powder diffraction patterns for defect-free spheres, disks, and rods, of hcp, fcc and ε-Co nanocrystals. In case of ε-Co spheres, the simulated and experimental patterns are qualitatively similar in terms of relative intensities and broadening of the peaks. The disk shaped samples show two prominent peaks in the diffraction patter, at 49º and 91º, which are enhanced as well in the simulations of the hcp disks. Diffraction patterns can be fit as a superposition of the hcp-disk and ε-sphere patterns, taking into account stacking faults, magnetic history of the sample and degree of packing of the disks, i.e., texture (not shown).

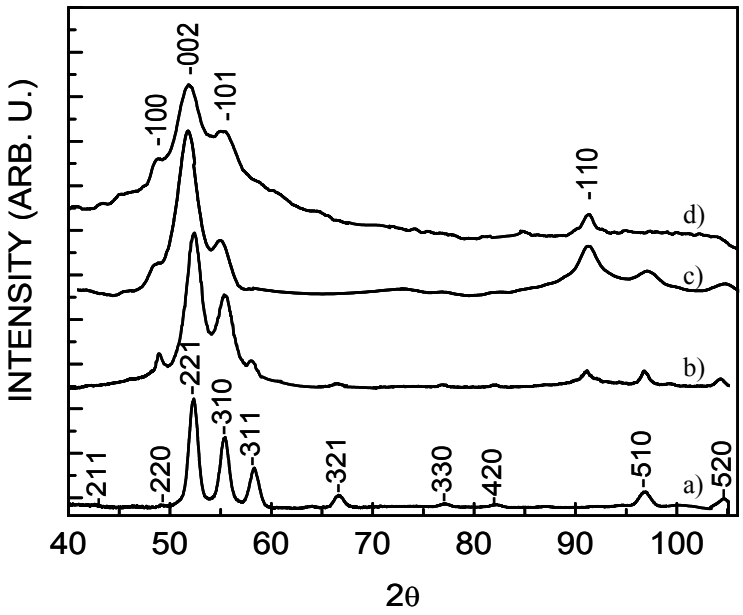

Fig.5. XRD patterns (bottom to top) of a) ε-Co spheres b) mixture of ε-Co spheres and hcp Co disks, c) another mixture, richer in hcp-disks, d) hcp disks obtained by magnetic fractioning of sample c). Grey arrows indicate the peaks which appear intensified when amines (and therefore disks) are present in solution.

Both TEM and XRD studies suggest that spheres are ε-Co single crystals, while disks show a textured hcp structure. HRTEM images show hexagonal symmetry and a lattice spacing of 2.17 Å (supplementary material). This value corresponds to the (100) planes of an hcp structure corroborating the XRD data that the short axis is the [001].

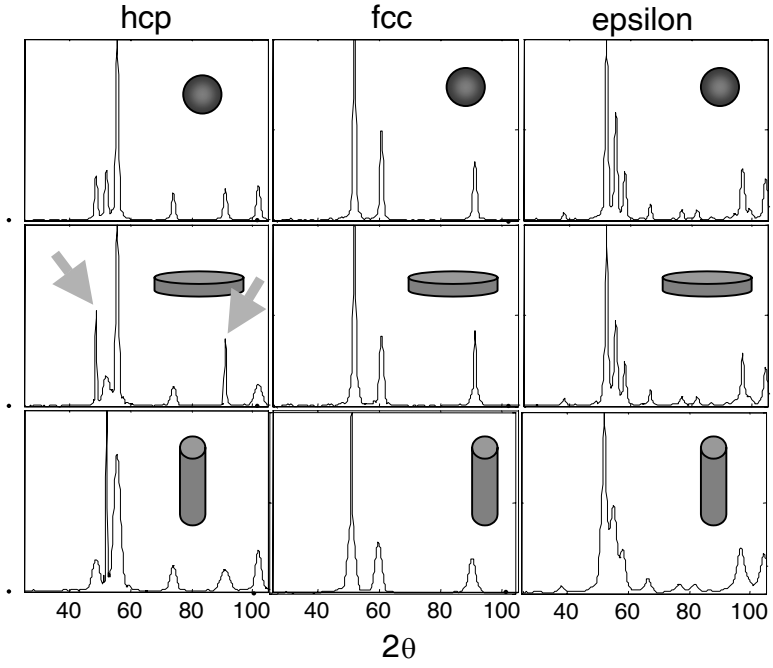

Fig. 6. Simulated XRD of defect-free Co hcp, fcc and epsilon spheres, disks and rods. First raw correspond to 11 nm diameter spheres, second to 4x20 nm disks and third, 20x4 rods. Grey arrows indicates the peaks which appear intensified when hcp-disks are simulated.

The length and diameter of the hcp-Co nanodisks can be controlled, primarily by variation of the reaction time following nucleation as well as by variation of the precursor to surfactant ratios. Figure 7 displays a set of experiments yielding progressively larger disks. The narrowest size distributions are obtained for medium sized (about 4x35 nm) disks. The average size of the smaller disks is about 2x4 nm and about 4x90 nm for the largest.

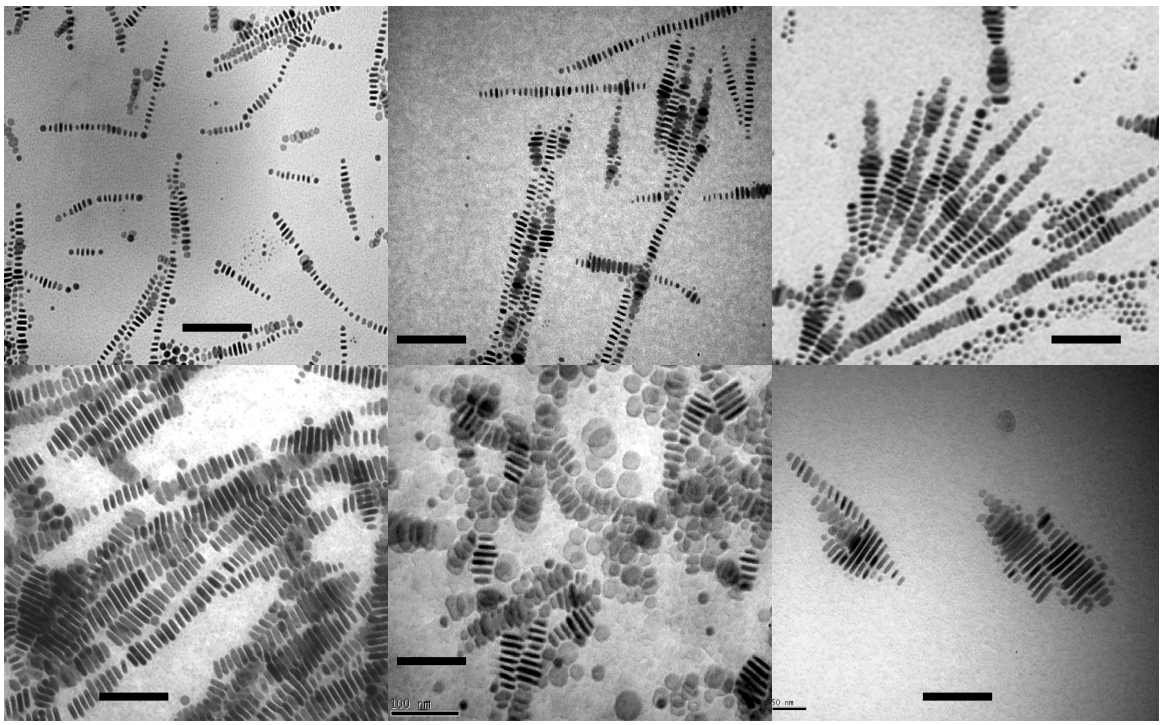

Fig.7. TEM of Co nanodisks as a function of disk size (left to right and up to down). Bars are 100 nm.

Magnetic nanodisks make close packed arrangements in one dimension that may become fairly large, extending over hundreds of nanocrystals, and these assemblies usually lie flat on a substrate. A tendency for parallel arrangement of the disk assemblies is observed (Fig.8 left) and it can be induced by applying an external magnetic field (Fig.8 right). Preliminary magnetic measurements of the nanodisk ferrofluids [15] showed a soft magnetic material with high magnetic moment and strong interactions, showing no hysteresis at room temperature. This indicates that the interactions are demagnetizing, and supports the idea that the disks are coupled antiferromagnetically (Fig.9).

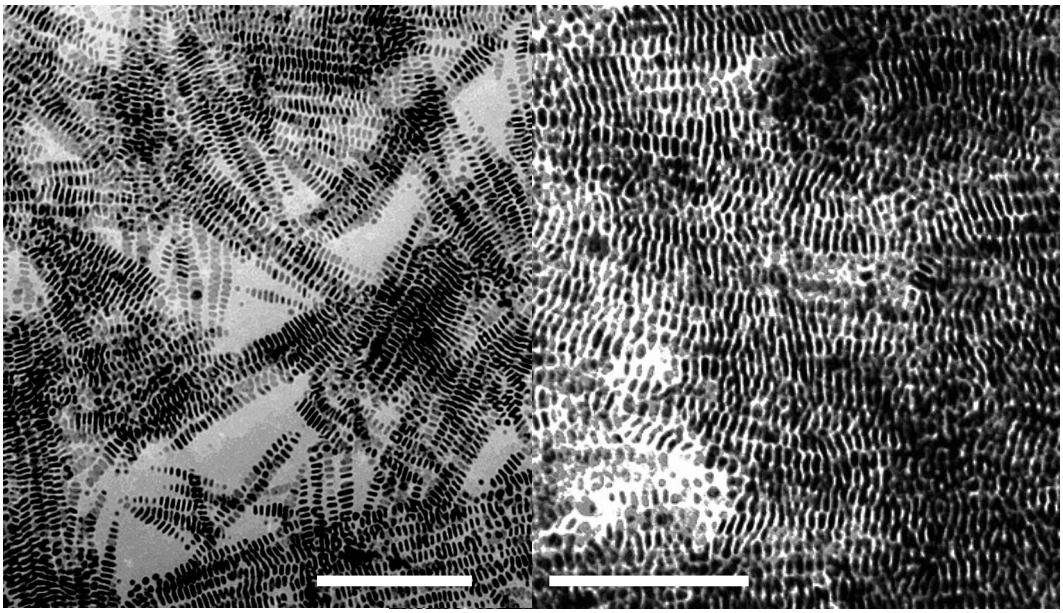

Fig.8. Co nanodisks self-assembled (left) and deposited under magnetic field (1 Tesla, right). Bar is 100 nm.

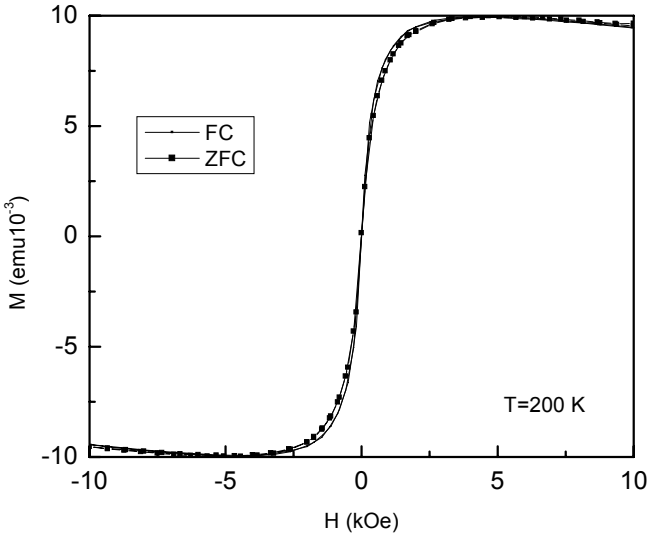

Fig.9. Hysteresis loop at 200 K after zero field cooling and 1 Tesla field cooling of a diluted Co nanodisk (4x35 nm) sample.

When the colloids are evaporated in the absence of field in more dilute conditions, disks also self-assemble (Fig. 10). While the smaller disks tend to lie

flat on the substrate more often, larger disks show a clear predisposition to stack and remain vertical to the substrate.

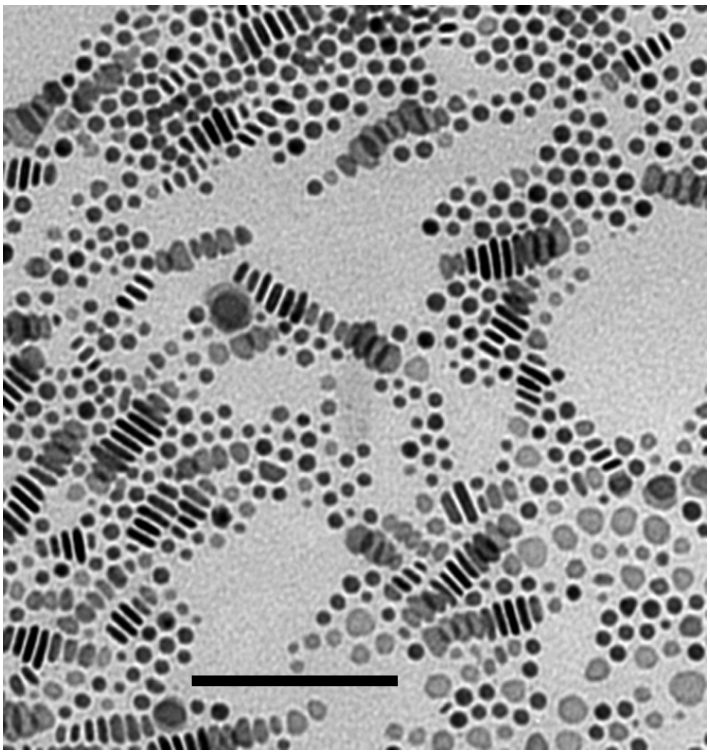

Fig.10. TEM of self assembled Co nanocrystals. Bar is 100 nm.

In the event of a large size distribution of disks, the disk assemblies consistently form in such a way that the larger disks are at the center of the ribbon. This is analogous to what has been observed in two-dimensional aggregates of poly-disperse spherical metallic nanocrystals [16]. The ribbons probably nucleate via aggregation of the largest disks first, and progressively smaller disks add to the ends, in a manner reminiscent of size-selective precipitation. Disks stay on edge or lie flat with small diameter variations, suggesting

that the magnetic and van der Waals interactions are of similar magnitude and close to k_BT.

Nanodisk solutions are stable black ferrofluids, susceptible to a magnetic field. Longer ribbons are observed after exposure of the ferrofluids to permanent magnets (and field gradients). Large assemblies slowly precipitate due to gravity. Ultrasound and vigorous shaking facilitates re-dissolution (and ribbon fragmentation). There are two special cases: i) in the case that the amine concentration is large (0.1 g/ml and up), the final solution separates into two phases with the particles and the excess of surfactant in an upper lighter phase, and ii) in the case of large ferromagnetic disks (larger than 30 to 40 nm in diameter), the magnetic interactions among them tend to spontaneously form large (hundreds of nm) superstructures that slowly precipitate. In both cases, the part of the solution without particles shows deep colored solutions due to the residual Co-surfactant complexes. Mild shaking instantaneously re-disperses the particles.

4. DISCUSSION

The Co system explored here displays many of the same features encountered previously in the growth of CdSe nanocrystals. These include the observation of size distribution focusing (spontaneous narrowing of the size distribution at high monomer concentration, provided monomer exchange is enabled) and shape control via selective adsorption of surfactants [17]. However,

there are also many important and interesting differences, and these are worth exploring.

First it is remarkable that in the case of hcp-Co, selective adsorption leads to a disk shape, while in wurtzite hexagonal CdSe grown in the presence of alkyl phophonic acids, phosphines, and phophine oxides, a rod shape is obtained. Evidently, alkyl amines act to inhibit the growth of the unique (001) face, relative to the growth of the perpendicular directions, the exact opposite of the role played by the phophonic acids in CdSe rod growth. The microscopic interactions between the crystallographic faces of hcp-Co and alkyl amines need to be investigated further. However, we do note that in the present experiments, the growth of Co nanocrystals in the presence of alkyl amines with $C_{12}<R<C_{18}$ (C_{12} being a 12 carbon chain) have been compared. The change in the length altered the results quantitatively but not qualitatively (lower disk and crystal yields are obtained with shorter chains, probably due to increase in atomic Co solubility), while R_3N (Trioctyl amine and Tributyl amine) completely spoiled the formation of disks. These observations suggest that i) the $–NH_2$ function is responsible for disk formation by selective adsorption, and ii) steric interactions among neighboring adsorbed molecules may have an impact on the growth rate of the (001) face.

The role of TOPO in these reactions is also very interesting. TOPO appears to promote atom exchange between the growing nanocrystals and the monomer reservoir, and is thus very important for size and shape control. The important effect of TOPO can be seen by the improvement in size distribution

when TOPO is added, as compared to the OA only case. While the presence of amines is enough to produce large amounts of disk shaped nanoparticles, the size dispersion of the disks is also considerably narrowed when TOPO is present.

Optimally, hcp Co disks should be faceted. Such hexagonal prisms are indeed observed, when the growth takes place in the presence of alkyl amines and TOPO (Fig.11). This further supports the idea of selective attachment where the more dense face is blocked by the amines and the others are left to grow. HRTEM of the prisms showed three (100, 010, 1-10) faces. Thus we find mixtures of regular hexagons and truncated triangles since both expose the same facets and angles. The existence of sharper triangle-like shapes (inset Fig.11, for more details see supplementary material) suggests that there may be more parameters affecting the growth. The transition from faceted to round disks results from selective etching of high-energy vertices, mainly performed by the TOPO in this case.

The fact that TOPO promotes atom exchange with the monomer reservoir also suggests that the surfactants play an important role by complexing with Co atoms, altering the nanoparticle-monomer equilibrium. This effect also occurs in the case of CdSe, where Cd is complexed by alkyl phosphonic acids (note that in both cases, CdSe and Co, it is important to utilize differential solubilities to separate product nanocrystals from left over molecular complex by-products; in the case of Co these complexes can be brightly colored and strongly paramagnetic).

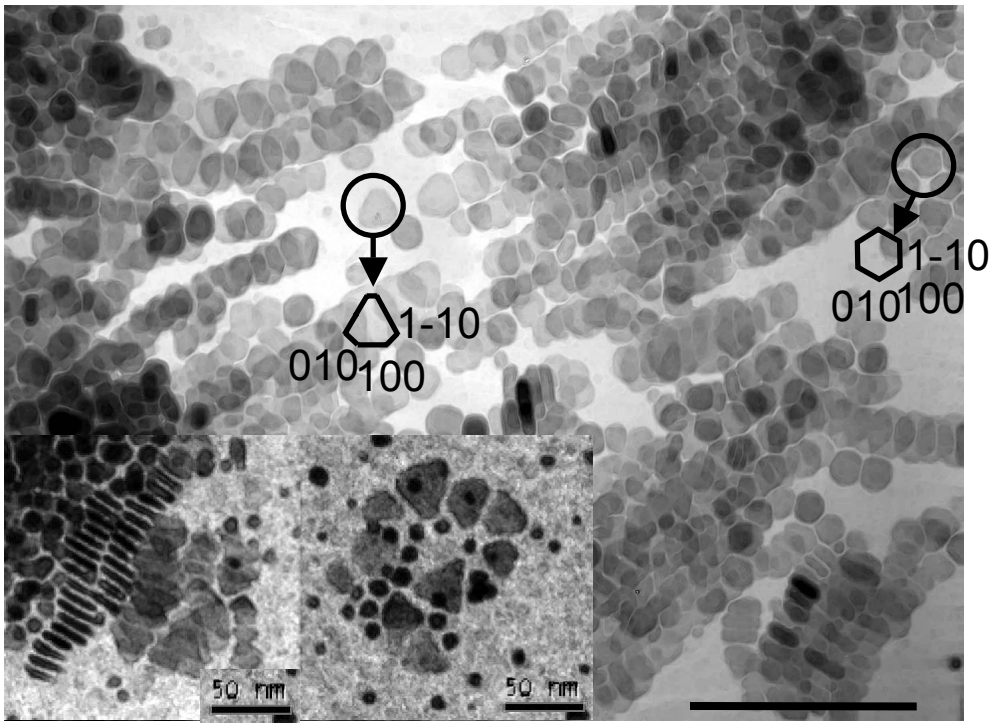

Fig.11. Flat Co nanocrystals. Labels represent hkl plane indices. Bar is 100 nm. Inset: Triangle-shaped Co nanocrystals.

The choice of solvent is also important, and DCB is particularly well suited for Co growth. More polar solvents (polar index>3, coordinating solvents) dissolve more of the precursor and complex with cobalt, producing beautiful, but definitely useless for our purposes, colored solutions (in the pink or the blue palette depending on the tetragonal or octagonal coordination of Co). Less polar solvents (toluene, hexane and pentane) have no effect on the reaction as long as the precursor can be dissolved.

The most critical moment of the reaction is injection, when decomposition, super-saturation, nucleation and rapid growth occur. In order to

get a monodisperse sample, rapid injection targeting half way between the flask walls and the center of the vortex created by the (vigorous) stirring is important. Upon injection of the $Co_2(CO)_8$ precursor, thermal decomposition of the carbonyl may happen faster than chemical homogenization and mixing of the solution. As a consequence, spherical nanoparticles may nucleate, regardless of the presence of the surfactant in the reaction medium (see Fig.2). Increasing the surfactant concentration is not always a good strategy to deal with this problem, because this alters the atomic Co solubility. Unfortunately, a homogeneous mixture of precursor, solvent and surfactant cannot be injected, because the surfactant reacts with the $Co_2(CO)_8$. Thus, a good solution is to inject both simultaneously but independently (otherwise, highly rapid and homogeneous stirring is needed).

In addition to the inherent interest of disks as a high surface nanocrystal, the magnetic properties are of considerable interest. Even the larger disks are expected to be single magnetic domains, since the break-up into magnetic domains in Co occurs at about 70 to 100 nm for spheres. In a disk shaped crystal the placement of the magnetic dipole along the short axis is very unlikely. Thus, the magnetic moment must be either blocked or rotating in the disk plane depending on size, anisotropy and temperature. In the latter case we will be dealing with two different rotating orientations, resulting in a magnetic phase that we could call two dimensional superparamagnetism (2DSP). Moreover, due to the non-ideal character of the material, there will always be a slight remanence, which may determine the rotating mode (clock-wise or counter-clock-wise), depending on whether the disks have been magnetized in or out of

plane. This could be used as a memory, presenting the natural advantage that as the magnetic moment is in a pseudo-superparamagnetic state (and still able to carry information), dipolar interactions among particles should be minimized and high recording density achieved in 2D flat Co nanodisks self assemblies.

Figure No.	Precursor Solution	Surfactants (dissolved in 15 ml DCB)	Collection time (sec)
1a	Standard	0.2 ml OA	300
1b	Standard	0.2 ml OA + 0.1 g TOPO	5
1c	Standard	0.2 ml OA + 0.1 g TOPO	300
2	Standard	0.9 g ODA	900
3,4,5,6b,8e	Standard	0.6 g ODA + 0.2 g TOPO	180
6a	Standard	0.6 g HDA + 0.2 g TOPO	300
8a	Dilute	0.9 g HDA + 0.1 ml OA	120
8b	Standard	1.5 g HDA + 0.1 ml OA	300
8c	Standard	0.9 g DDA + 0.1 ml OA	300
8d	Standard	0.9 g ODA + 0.1 ml OA	600
8f	Standard	1.6 g ODA + 0.1 ml OA + 0.05 g TOPO	720
9, 10	Small	0.45 g HDA + 0.05 ml OA	600
11	Standard	0.9 g HDA + 0.2 ml OA	600
12, 13	Standard	0.6 g HDA + 0.2 g TOPO	120

Table 1. Surfactant mixtures employed Precursor solution was injected into the flask containing surfactant/DCB mixture refluxing at ~ 182 ºC. 'Standard' refers to a solution of 0.54 g $Co_2(CO)_8$ in 3 ml DCB. 'Dilute' refers to a solution of 0.27 g $Co_2(CO)_8$ in 3 ml DCB. 'Small' refers to a solution of 0.27 g $Co_2(CO)_8$ in 1.5 ml DCB.

ACKNOWLEDGMENT

This work was supported by the Director, Office of Energy Research, Office of Science, Divisions of Materials and Chemical Sciences of the U.S. Department of Energy under contract no. DE-AC03-76SF00098 and NIH National Center for Research Resources, grant no. 1 R01 RR-14891-01. D.Z. thanks FAPESP (proc. 99/08603-7 and 01/07715-8) for financial support. NCEM/LBL Berkeley-CA and LME/LNLS Campinas-Brazil are acknowledged for the use of the TEMs.

REFERENCES

(1) See for example J.T. Hu, L.S. Li, W.D. Yang, L Manna, L.W. Wang, A.P. Alivisatos *Science* **2001**, *292* , 2060-2063

(2) Timothy J. Trentler, Kathleen M. Hickman, Subhash C. Goel, Ann M. Viano, Patrick C. Gibbons, and William E. Buhro *Science* **1995**, *270*, 1791.

(3) Pan, Z.W.; Dai, Z.R.; Wang, Z.L. *Science* **2001**, *291*, 1947.

(4) Urban, J. J.; Yun, W.S.; Gu, Q.; Park, H. *J. Am. Chem. Soc.* **2002**, *124*, 1186.

(5) Peng, Z.A.; Peng, X. *J. Am. Chem. Soc.* **2001**, *123*, 1389.

(6) Banfield, J.F.; Welch, S.A.; Hengzhong Zhang; Ebert, T.T.; Penn, R.L. *Science* **2000**, *289*, 751.

(7) Pacholski, C.; Kornowski A.; Weller, H. *Angew. Chem. Int. Ed.* **2002**, *41*, 1188.

(8) Bruno Chaudret, personal communication.

(9) Park, S.J.; Kim, S.; Lee, S.; Khim, Z.G.; Char, K.; Hyeon, T. *J. Am. Chem. Soc.* **2000**, *122*, 8581.

(10) Jin R.; Cao, Y.; Mirkin, C.A.; Kelly, K.L.; Schatz, G.C.; Zheng, J.G. *Science* **2001**, *294*, 1901; Klausen S. N., Lingard P.A., Lefmann K., Bodker F., Morup, S. *Phys. Stat. Sol.* **2002**, *189*, 1039.

(11) Dinega D.P.; Bawendi, M.G. *Angew. Chem. Int. Ed.* **1999**, *38*, 1788;

(12) Murray, C.B.; Shouheng Sun, *J. Appl. Phys.* **1999**, *85*, 4325-4330

(13) Puntes V.F.; Krishnan K.M.; Alivisatos A.P. *Science* **2001**, *291*, 2115.

(14) Suvanto, S.; Pakkanen, T.A.; Backman, L. *Appl. Catal. A: General* **1999**, *177*, 25.

(15) magnetic measurements of the precipitated powder and self assembled monolayers may be found in : Victor F Puntes, A. P. Alivisatos and K. Krishnan, *Appl. Phys. Lett.* **2001**, *78*, 2187; Victor F Puntes and K. Krishnan IEEE Trans. on Magn. **2001**, *37*, 2210.

(16) Pamela C. Ohara, Daniel V. Leff, James R. Heath, and William M. Gelbart, *Phys. Rev. Lett.* 1995, *75*, 3466.

(17) Manna, L., Scher E.C.; Alivisatos A.P. *J. Am. Chem. Soc.* **2000**, *122*, 12700.

Table of Contents Figure

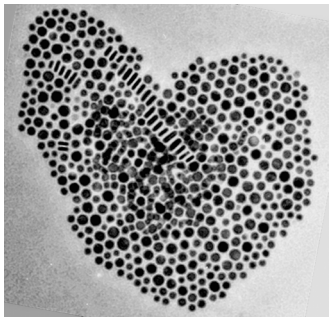

Flat and standing self assembled Co nanodisks of 25 nm in average diameter.